CELL BIOLOGY

The orphan nuclear receptor LRH-1/NR5a2 critically regulates T cell functions

Carina Seitz[1], Juan Huang[1,2], Anna-Lena Geiselhöringer[1], Pamela Galbani-Bianchi[3], Svenja Michalek[1], Truong San Phan[1], Cindy Reinhold[1], Lea Dietrich[1], Christian Schmidt[1], Nadia Corazza[3], M. Eugenia Delgado[1], Theresa Schnalzger[1], Kristina Schoonjans[4], Thomas Brunner[1]*

LRH-1 (liver receptor homolog-1/NR5a2) is an orphan nuclear receptor, which regulates glucose and lipid metabolism, as well as intestinal inflammation via the transcriptional control of intestinal glucocorticoid synthesis. Predominantly expressed in epithelial cells, its expression and role in immune cells are presently enigmatic. LRH-1 was found to be induced in immature and mature T lymphocytes upon stimulation. T cell–specific deletion of LRH-1 causes a drastic loss of mature peripheral T cells. LRH-1–depleted CD4$^+$ T cells exert strongly reduced activation-induced proliferation in vitro and in vivo and fail to mount immune responses against model antigens and to induce experimental intestinal inflammation. Similarly, LRH-1–deficient cytotoxic CD8$^+$ T cells fail to control viral infections. This study describes a novel and critical role of LRH-1 in T cell maturation, functions, and immopathologies and proposes LRH-1 as an emerging pharmacological target in the treatment of T cell–mediated inflammatory diseases.

INTRODUCTION

An interaction between dietary and microbial-derived lipids and the immune system has been suggested for a long time. Food- and microbiome-derived lipids regulate host metabolism and thereby obesity, which, in turn, promotes inflammation and associated diseases, such as type 2 diabetes and cancer [reviewed in (*1*) and (*2*)]. Best characterized is the role of short-chain fatty acids, such as butyrate and acetate, derived from bacterial digestion of food (*3*). However, also longer chain fatty acids and phospholipids are known to be taken up by the gastrointestinal tract and to regulate immunological processes [reviewed in (*4*)]. The underlying molecular mechanisms remain, so far, largely unexplored.

Lipid molecules are often bound and sensed by a large group of transcription factors, the nuclear receptor family. Nuclear receptors play important roles in various developmental, metabolic, and inflammatory processes. Lipid ligand binding promotes their transcriptional activation via coactivator recruitment [reviewed in (*5*)]. Best characterized is the group of steroid hormone receptors, which bind cholesterol derivatives, such as sex hormones, aldosterone, and glucocorticoids. In particular, the glucocorticoid receptor is known to exert potent immunoregulatory activities, providing the basis for the efficient therapeutic use of synthetic glucocorticoids in the treatment of inflammatory processes (*6*). Endogenous glucocorticoids are produced not only in the adrenal glands but also by extra-adrenal sources, such as the thymus, skin, lung, and intestine (*7*). Thus, we have previously shown that the intestinal epithelium is an important source of glucocorticoids and that intestinal glucocorticoids critically contribute to the regulation of local immune homeostasis (*8*–*11*).

The synthesis of immunoregulatory glucocorticoids in the intestinal epithelium is critically controlled by the nuclear receptor liver receptor homolog-1 (LRH-1/NR5a2) (*9*, *10*), which belongs to the fushi tarazu family of transcription factors [reviewed in (*12*)]. Deletion of LRH-1 in the intestinal epithelium predisposes mice to development of intestinal inflammation due to the absence of local glucocorticoid synthesis (*9*). Furthermore, studies in patients with ulcerative colitis and Crohn's disease revealed a clear negative correlation between LRH-1, intestinal glucocorticoids, and intestinal inflammation (*9*). LRH-1 is considered an orphan nuclear receptor, as no endogenous ligand has been identified so far. Various reports have, however, highlighted the fact that LRH-1 binds phospholipids, lipids, and lipophilic chemical compounds, resulting in transcriptional activation of the nuclear receptor (*13*, *14*).

Although intestinal LRH-1 regulates immune cells via immunoregulatory glucocorticoids (*10*), little is currently known about the expression of LRH-1 in the hematopoietic system. Recently, a role of LRH-1 in the differentiation of macrophage subpopulations and the development of anti-infectious effector functions has been demonstrated (*15*). Similarly, we were able to demonstrate that LRH-1 contributes to the transcriptional control of Fas (CD95) ligand expression and associated effector functions in CD4$^+$ T lymphocytes (*16*). However, the expression and role of LRH-1 in cells of the T cell lineage are currently unexplored and enigmatic. Here, we demonstrate a novel and direct role of LRH-1 in immune regulation. LRH-1 is expressed in murine thymocytes and mature T lymphocytes, and stimulation of cells further induces LRH-1 expression. CD4 promoter–driven deletion of LRH-1 at the CD4/CD8 double-positive stage in the thymus has only a minor impact on thymocyte maturation but severely reduces the number of peripheral T cells. While LRH-1–deficient T cells show normal signs of early T cell activation, they exert strongly reduced activation-induced proliferation in vitro and in vivo. LRH-1 deficiency severely impairs T cell responses and antibody production in vivo and abrogates CD4 T cell–mediated experimental colitis. Upon viral infection, LRH-1–deficient CD8$^+$ T cells readily become activated and produce excessive amounts of cytokines yet fail to control virus expansion. This study demonstrates a critical role of LRH-1 in T cell maturation and the regulation of T cell homeostasis, T cell expansion, and effector functions. Furthermore, our study proposes LRH-1 as an emerging new target in the treatment of T cell–mediated inflammatory diseases.

[1]Division of Biochemical Pharmacology, Department of Biology, University of Konstanz, Konstanz, Germany. [2]Institute of Preventive Veterinary Medicine, Sichuan Agricultural University, Sichuan, P.R. China. [3]Experimental Pathology, Institute of Pathology, University of Bern, Bern, Switzerland. [4]Laboratory of Metabolic Signaling, Institute of Bioengineering, School of Life Sciences, École Polytechnique Fédérale de Lausanne, Lausanne, Switzerland.
*Corresponding author. Email: thomas.brunner@uni-konstanz.de

RESULTS

LRH-1 deletion results in reduced mature T cells

Because of the lack of information concerning the expression of LRH-1 in hematopoietic cells, we first investigated its gene expression profile in different lymphatic tissues (fig. S1A) and immature (fig. S1B) and mature T cell subsets (fig. S1C). This revealed that *Nr5a2* mRNA expression was low but detectable in all immature and mature T cell subsets of C57BL/6 wild-type mice (fig. S1, B and C) and in human peripheral blood mononuclear cells (PBMCs) (fig. S1D).

To address the role of LRH-1 in T lymphocytes, we next generated T cell–specific LRH-1–deficient mice using CD4 promoter–driven Cre recombinase expression [$Nr5a2^{L2/L2}$ CD4-Cre, conditional knockout (cKO)]. As CD4 expression is first observed at the $CD4^+CD8^+$ stage of thymocyte maturation, we compared the thymi of cKO and control (L2/L2) animals but found no difference in size (fig. S2A), weight (fig. S2B), or cellularity (fig. S2C). Only a mild reduction of $CD4^+$ and $CD4^+CD8^+$ and a corresponding increase in $CD4^-CD8^-$ thymocytes were observed (fig. S2D).

When analyzing secondary lymphatic organs, we observed that the spleen of cKO animals was significantly reduced in size (Fig. 1A), organ weight (Fig. 1B), and cell numbers (Fig. 1C). Unexpectedly, $CD8^+$ T cells were reduced by approximately 50%, and $CD4^+$ lymphocytes were reduced by almost 80% in cKO spleens (Fig. 1D). In line with the significant loss of splenic $CD3^+$ T cells (Fig. 1E), the relative number of $B220^+$ B cells was increased (Fig. 1F) and no difference was observed for $NK1.1^+$ (Fig. 1G) in cKO animals. The relative loss of $CD4^+$ and $CD8^+$

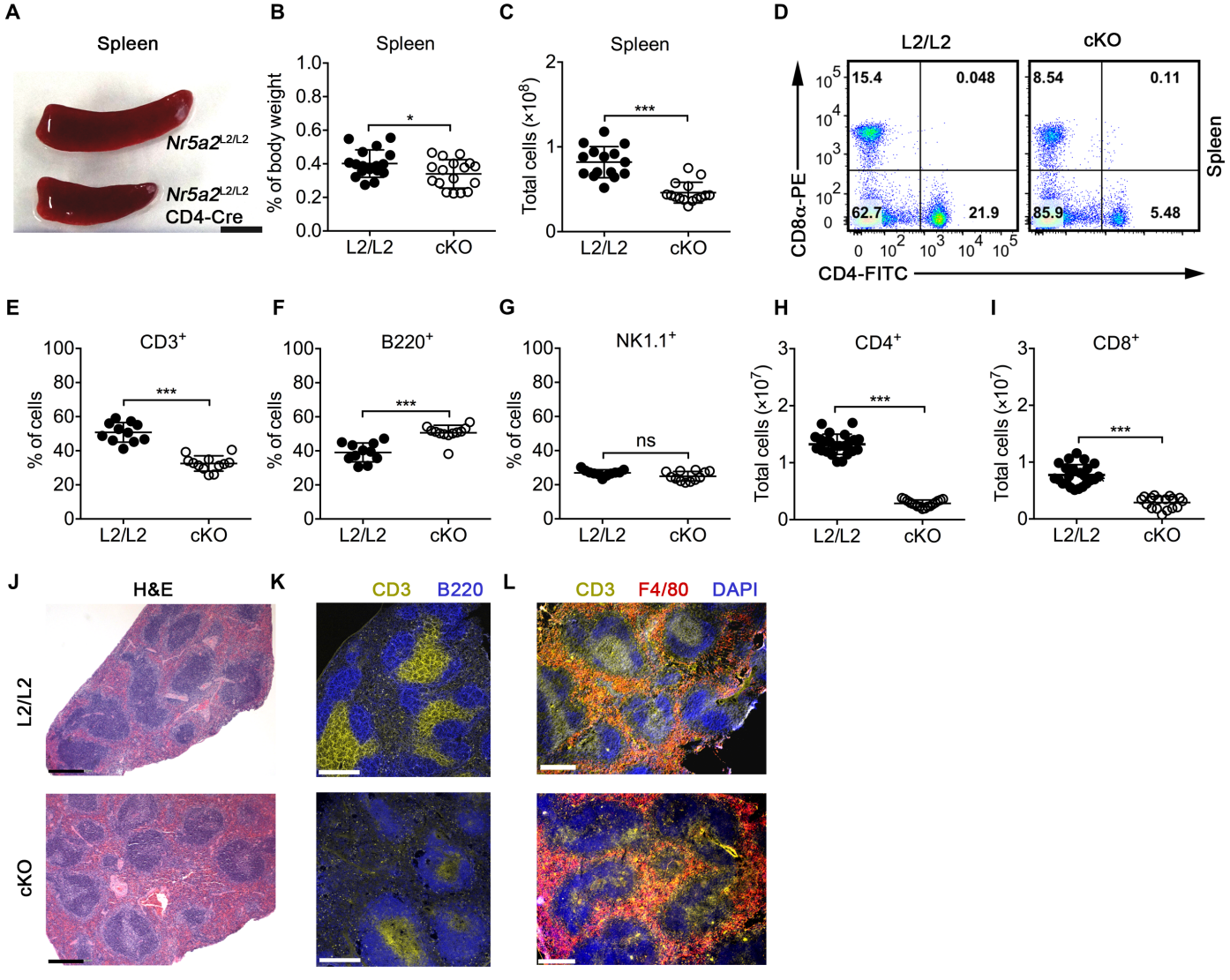

Fig. 1. Deletion of *Nr5a2* leads to loss of mature T lymphocytes. (**A**) Representative picture of $Nr5a2^{L2/L2}$ (L2/L2, ctrl) and $Nr5a2^{L2/L2}$ CD4-Cre (cKO) spleens. ctrl, control. (**B**) Spleen organ weight relative to body weight (L2/L2, $n = 17$; cKO, $n = 18$ mice). (**C**) Spleen cellularity ($n = 15$). (**D**) Representative density plots of splenic $CD4^+$ and $CD8^+$ cells. The numbers indicate the percentage of cells. PE, phycoerythrin; FITC, fluorescein isothiocyanate. (**E** to **G**) Relative distribution of splenic $CD3^+$ (E), $B220^+$ (F), or $NK1.1^+$ (G) $CD3^+$ cells analyzed by flow cytometry (L2/L2, $n = 11$ mice; cKO, $n = 12$ mice per group). (**H** and **I**) Absolute numbers of splenic $CD3^+CD4^+$ and $CD3^+CD8^+$ T lymphocytes (L2/L2, $n = 23$; cKO, $n = 17$). (**J**) Representative hematoxylin and eosin (H&E) staining of L2/L2 or cKO spleens. (**K**) Representative immunohistology for CD3 (yellow) and B220 (blue) expression. (**L**) Representative staining for CD3ε (yellow), F4/80 (red), and 4′,6-diamidino-2-phenylindole (DAPI) (blue). Scale bars, 0.5 cm (A) and 300 μm (J to L). Mean values ± SD and individual values are shown in each graph. $^*P < 0.05$ and $^{***}P < 0.001$. ns, not significant. Photo credit: Carina Seitz, University of Konstanz.

T cells was confirmed when analyzing total cell numbers (Fig. 1, H and I). Comparable changes in $CD4^+$ and $CD8^+$ T cell numbers were found in axial (fig. S3, A to F) and mesenteric lymph nodes (fig. S3, G to L).

Because of the strong phenotype of LRH-1 deletion in mature T cell distribution, we next analyzed the splenic architecture. Histological analysis revealed obvious changes in the structure of white pulp follicles, which were more compact and with a lighter core, suggesting a reduced cell density (Fig. 1J). Immunohistological detection of B and T lymphocytes confirmed a reduced size of the T cell zone (Fig. 1K), while the overall distribution of B cell follicles and marginal zone macrophages (Fig. 1L) was not altered.

As CD4 promoter–driven deletion of LRH-1 had a stronger impact on numbers of peripheral $CD4^+$ than $CD8^+$ T cells, the question whether Cre-mediated deletion was less effective in $CD8^+$ T cells arose. We thus used a Tomato-membrane green fluorescent protein (GFP) (mTmG) double-fluorescent Cre reporter mouse line, in which successful Cre-mediated recombination results in green fluorescence of cells (*17*). As expected, immature $CD4^-CD8^-$ thymocytes showed very low GFP levels and, hence, minimal LRH-1 deletion (fig. S4A), while the deletion was nearly complete in more mature $CD4^+CD8^+$ thymocytes (fig. S4B), as well as in thymic, splenic, axial, and mesenteric $CD4^+$ and $CD8^+$ subsets (fig. S4, C, D, and F to H). Microscopic analysis of spleen sections confirmed specific LRH-1 deletion (GFP^+) in the T cell area (fig. S4E). Overall, the rate of GFP^+ $CD8^+$ T cells was slightly lower, however, with 80 to 90% still almost complete.

Sensitivity of LRH-1–deficient T cells to apoptosis induction

To understand the underlying cause of LRH-1 deletion-mediated loss in peripheral T cells, we investigated the apoptosis sensitivity of cKO T cells. Enhanced basal cell death was observed in cKO thymocytes (fig. S5, A to D) and splenocytes (fig. S6, A to D), while their response toward dexamethasone, etoposide, staurosporine, or plate-bound anti-CD3 promoting activation-induced cell death was comparable to the L2/L2 controls (figs. S5, A to D, and S6, A to D). Hence, increased stimulus-induced cell death does not appear to account for the selective loss of peripheral T cells in cKO mice.

As proliferating T cells are more sensitive to apoptosis-inducing agents, especially to activation-induced cell death (*18*), we addressed apoptosis induction in concanavalin A (ConA)–induced T cell blasts. Unexpectedly, cKO $CD4^+$ cells and, to a lesser extent, $CD8^+$ T cells failed to expand under these conditions and rather died, leading to approximately 80% basal cell death. This time-dependent increase in cell death of $CD4^+$ cKO T cells was observed after ConA stimulation (fig. S6E) and anti-CD3/anti-CD28 treatment (fig. S6F).

LRH-1–deficient T cells are not anergic

Because of the increased cell death in response to mitogenic stimuli, we tested the hypothesis that LRH-1–deficient T cells fail to become activated after T cell receptor stimulation. While the activation induced up-regulation of the early activation markers CD69 and CD25 was slightly but significantly lower and slower in $CD4^+$ and $CD8^+$ cKO T cells, both responded to T cell activation by up-regulating both activation markers (Fig. 2, A and B).

To further exclude anergy as a cause of reduced numbers of LRH-1–deficient T cells, we analyzed their capability of effector cytokine expression and secretion. Interferon-γ (IFN-γ) secretion was detected in purified $CD4^+$ and $CD8^+$ T cells of both cKO and L2/L2 mice with even much higher levels in cKO T cells (Fig. 2C). Similar results were obtained for interleukin-2 (IL-2)

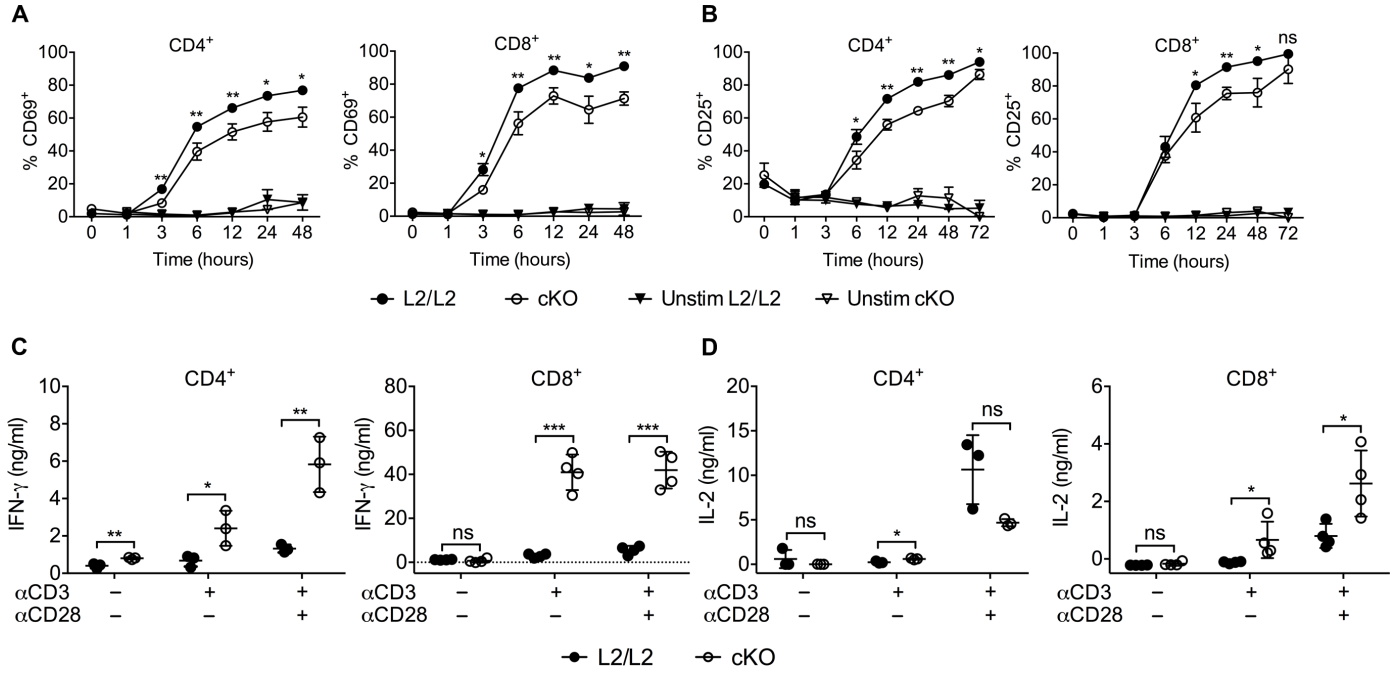

Fig. 2. LRH-1–deficient T cells are not anergic. (**A** and **B**) Up-regulation of the early activation marker CD69 (A) and CD25 (B) in unstimulated (unstim) or anti-CD3 (3 μg/ml) and anti-CD28 (1 μg/ml) (stim) $CD4^+$ or $CD8^+$ splenic T cells ($n = 3$ mice). (**C** and **D**) Production of interferon-γ (IFN-γ) (C) or interleukin-2 (IL-2) (D) in purified $CD4^+$ or $CD8^+$ splenic T cells. Cells were stimulated as indicated for 48 hours, and cytokine secretion was determined by enzyme-linked immunosorbent assay (ELISA) ($n = 4$ mice). Mean values ± SD of triplicates or quadriplicates of representative experiments are shown. $^*P < 0.05$, $^{**}P < 0.01$, and $^{***}P < 0.001$.

expression (Fig. 2D), confirming that LRH-1 deletion does not impair T cell activation.

Impaired activation-induced proliferation in LRH-1–deficient T cells

As cKO T cells were neither hypersensitive to stimulus-induced apoptosis induction nor anergic, we hypothesized that LRH-1 deficiency directly affects T cell proliferation and expansion. Hence, we investigated the effect of mitogenic stimuli on *Nr5a2* mRNA expression and found a significant increase in mouse splenocytes (Fig. 3A) and human PBMCs (Fig. 3B). Activation-induced *Nr5a2* expression closely correlated with cell cycle progression, as monitored by the mRNA expression of cyclins (Fig. 3, C to E). As expected, expression of *Myc*, a direct regulator of the cell cycle machinery, was induced very early after activation (Fig. 3C). *Nr5a2* expression was induced soon after stimulation with a peak at 3 to 6 hours (Fig. 3D), followed by cyclin E1 (*Cdne1*) (Fig. 3E), a transcriptional target of LRH-1 (*19*). We further observed increased LRH-1 promoter activation in response to mitogenic stimulation in Jurkat lT cells (Fig. 3F), whereas serum withdrawal decreased LRH-1 promoter activity (Fig. 3G).

We next tracked spleen cell division by carboxyfluorescein diacetate succinimidyl ester (CFSE) dilution assay and observed a prominent reduction in LRH-1–deficient $CD4^+$ T cells, while proliferation was not reduced or delayed in the $CD8^+$ subset (Fig. 4, A and B). To confirm a role of LRH-1 in T cell proliferation, specific pharmacological inhibitors were applied to mimic the loss of LRH-1 protein. While the LRH-1 inhibitor 3d2 (*20*) resulted in significant inhibition of cell division even for the lowest concentrations, the inactive control substance cd7 (*20*) did not (Fig. 4, C and D). 3d2 was also able to inhibit $CD8^+$ T cell proliferation, although higher concentrations were necessary (Fig. 4D). An inhibition of T cell proliferation was also observed with another LRH-1 inhibitor, SR1848 (Fig. 4E) (*21*). Reduced activation-induced proliferation of LRH-1–deficient T cells was confirmed by ^{3}H-thymidine incorporation of highly purified $CD4^+$ and $CD8^+$ T cells (Fig. 4F), suggesting that also in the absence of splenic accessory cells, $CD8^+$ T cells depend on LRH-1. To understand the molecular basis of this reduced proliferation, we analyzed the expression of cell cycle–regulating target genes of LRH-1, i.e., c-Myc (*Myc*) and cyclin E1 (*Cdne1*) (*19*, *22*). In agreement with the reduced proliferation observed in activated cKO T cells, a reduced induction *Myc* and *Cdne1* expression was seen in $CD4^+$ cKO T cells and reduced *Myc* expression in $CD8^+$ T cells (Fig. 4, G and H).

We next assessed the role of LRH-1 in homeostatic T cell expansion in vivo by adoptively transferring purified cKO or L2/L2 T cells into lymphopenic recipient mice. Analysis of spleen and mesenteric lymph nodes revealed major defects of $CD4^+$ cKO T cell expansion and reduced repopulation of LRH-1–deficient $CD8^+$ T cells (fig. S7, A and B). To further monitor activation-induced T cell expansion in vivo, we analyzed the ex vivo T cell restimulation of ovalbumin-immunized mice. While an antigen-dependent proliferation of T cells was detectable in immunized L2/L2 mice, no ex vivo proliferation was seen in T cells from cKO mice (fig. S8, A and B). In addition to the lack of ovalbumin-induced T cell expansion in vivo, a massive reduction of anti-ovalbumin immunoglobulins in the sera of cKO mice was observed, revealing defects in T cell–dependent B cell activation (fig. S8C).

Impaired colitis induction by LRH-1–deficient T cells

To test the consequence of impaired proliferation in a T cell–dependent pathogenesis model in vivo, we used the T cell transfer colitis model. In this model, naïve $CD4^+$ $CD45Rb^{hi}$ T cells are transferred into

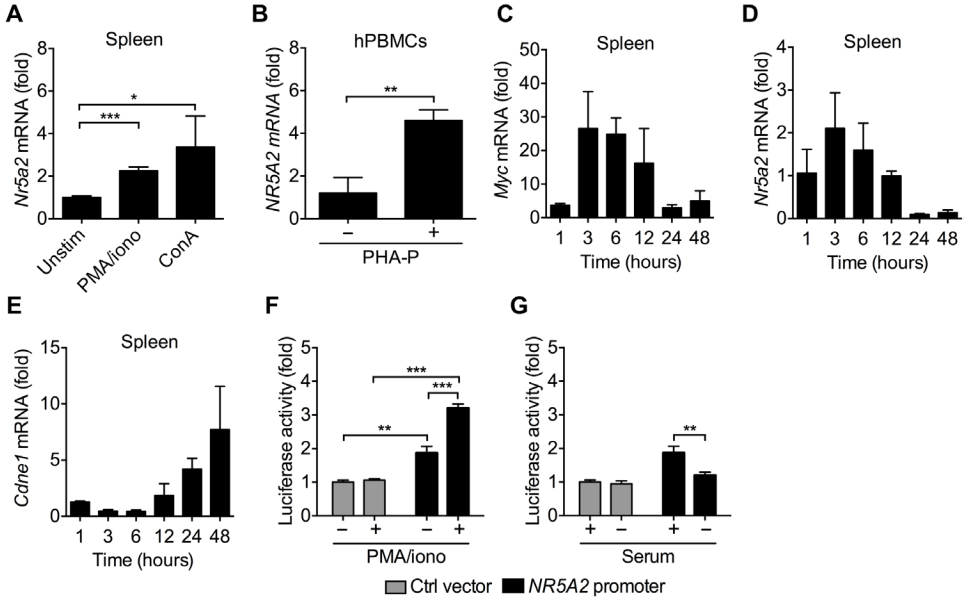

Fig. 3. *Nr5a2* expression is up-regulated upon stimulation. (**A**) *Nr5a2* mRNA expression in wild-type spleenocytes after 3 hours of phorbol myristate acetate (PMA) and ionomycin (iono) or ConA stimulation, normalized to unstimulated control ($n = 3$ mice per group). (**B**) *NR5A2* mRNA expression in human PBMCs (hPBMCs) after stimulation with phytohemagglutinin (PHA-P) for 3 hours ($n = 3$ biological replicates). (**C** to **E**) Kinetics of (C) *Myc*, (D) *Nr5a2*, and (E) *Cdne1* expression in splenocytes after anti-CD3/anti-CD28 stimulation normalized to unstimulated control ($n = 3$ mice). (**F**) Induction of *NR5A2* promoter activity in Jurkat lT cells after stimulation with PMA and ionomycin. One representative experiment of five is shown ($n = 3$ technical replicates). (**G**) Effect of serum deprivation on NR5A2 promoter activity. One of three representative experiments is shown ($n = 3$ technical replicates). $^*P < 0.05$, $^{**}P < 0.01$, and $^{***}P < 0.001$.

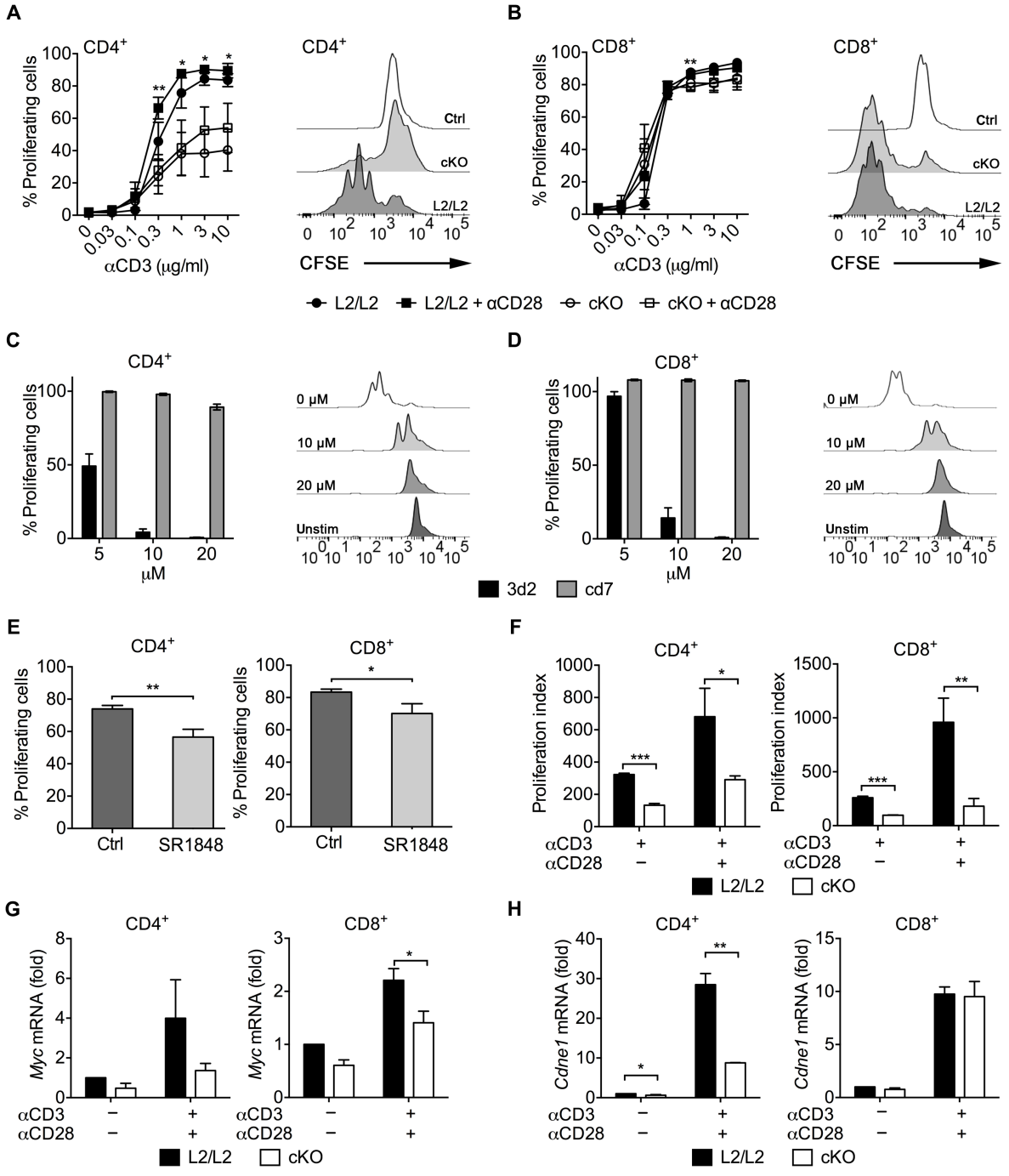

Fig. 4. Impaired cell proliferation in LRH-1–deficient T cells. (**A** and **B**) Cell proliferation in response to anti-CD3 ± anti-CD28 stimulation of splenic CD4$^+$ and CD8$^+$ T cells was analyzed by CFSE dilution after 72 hours. Mean values ± SD of three individual experiments are shown. (**C** and **D**) Spleen cells were stimulated with anti-CD3 and anti-CD28 in the presence or absence of the LRH-1 antagonist 3d2 or control substance cd7 at indicated concentrations, and proliferation was analyzed by CFSE dilution at 72 hours. Values were normalized to stimulated cells without inhibitors ($n = 3$ mice). (**E**) Splenocytes were treated with or without the LRH-1 inhibitor SR1848 and stimulated with anti-CD3/anti-CD28; cell proliferation was analyzed by CFSE dilution at 72 hours ($n = 3$ mice). (**F**) Activation-induced ^{3}H-thymidine incorporation in purified CD4$^+$ and CD8$^+$ splenic T cells after 72 hours, normalized to unstimulated cells. Mean values ± SD of a representative experiment are shown ($n = 5$ experiments). (**G** and **H**) Activation-induced *Myc* (G) and *Cdne1* (H) mRNA expression in purified CD4$^+$ and CD8$^+$ splenic T cells after 24 hours. *$P < 0.05$, **$P < 0.01$, and ***$P < 0.001$.

lymphopenic Rag1$^{-/-}$ mice, where their uncontrolled activation by gut microbiota leads to subsequent colitis induction (Fig. 5A) (*23*, *24*). While transfer of L2/L2 T cells resulted in a time-dependent loss of body weight (Fig. 5B) and massive colonic inflammation, cKO T cell transfer failed to promote body weight loss and caused significantly less colonic inflammation (Fig. 5, C to E). The reduced colitis induction of cKO donor cells observed was paralleled by diminished T cell expansion and repopulation of spleen and mesenteric lymph

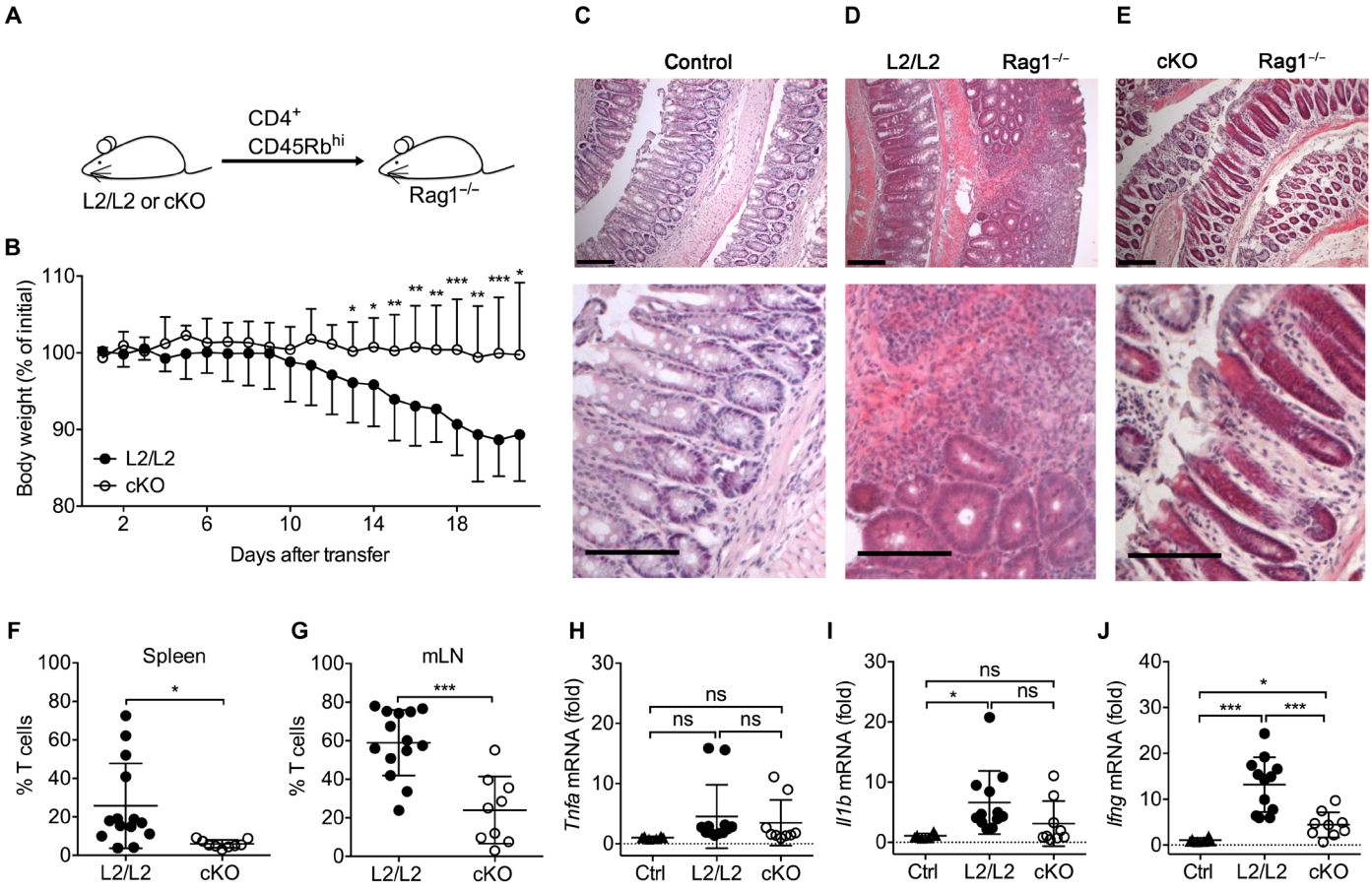

Fig. 5. Impaired colitis induction by LRH-1–deficient CD4$^+$T cells. (**A**) Scheme of transfer colitis induction in Rag1$^{-/-}$ recipient mice. (**B**) Colitis-induced loss of body weight (L2/L2 donor, $n = 14$; cKO donor, $n = 9$). (**C** to **E**) Representative histologies of colon samples from untreated Rag1$^{-/-}$ recipient mice (C) or after transfer of naïve L2/L2 (D) or cKO T cells (E). Top panels: Lower magnification. Bottom panels: Higher magnification. Scale bars, 150 μm. (**F** and **G**) Repopulation of spleen (F) or mesenteric lymph node (mLN) (G) by naïve L2/L2 or cKO T cells. (**H** to **J**) mRNA expression levels of the proinflammatory cytokines tumor necrosis factor–α (H), IL-1β (I), and IFN-γ (J) in colon samples or control recipients or recipients transferred with L2/L2 or cKO T cells. Mean ± SD and individual data points of $n = 9$ to 14 mice are shown. *$P < 0.05$, **$P < 0.01$, and ***$P < 0.001$.

node (Fig. 5, F and G) and reduced IFN-γ expression in the colon of Rag1-deficient recipient mice (Fig. 5. H to J).

Reduced regulatory function of LRH-1–deficient T cells

To further study the putative role of LRH-1 in regulatory T cells (T_{regs}), we conducted a colitis protection experiment. While naïve CD4$^+$ CD45Rb^{hi} T cells are able to infiltrate colonic tissue and induce colitis upon transfer into lymphopenic mice, cotransfer of CD4$^+$ CD45Rb^{lo} T cells results in pronounced protection from colitis induction, mediated by T_{regs} in this T cell population (fig. S9A) (*24*, *25*). Accordingly, the transfer of Ly5.1$^+$ CD4$^+$ CD45Rb^{hi} T cells caused pronounced colitis, accompanied by body weight loss (fig. S9B) and colonic inflammation (fig. S9C), whereas the cotransfer of CD4$^+$ CD45Rb^{lo} T cells from L2/L2 mice resulted in the restoration of body weight loss (fig. S9B) and reduced colonic inflammation (fig. S9D). In marked contrast, sort-purified cKO CD4$^+$ CD45Rb^{lo} T cells were unable to attenuate disease development (fig. S9, B and E). Along these lines, reduced regulatory cKO donor T cell numbers were found in spleen (fig. S9F) and mesenteric lymph nodes (fig. S9G) of recipient mice, suggesting that the disturbed protective functions of cKO T cells resulted from reduced in vivo expansion. While L2/L2 T_{regs} were able to significantly reduce colonic *Ifng* mRNA expression and cKO T cells failed to do so (fig. S9H), there was no difference in *Il1b* expression (fig. S9I), but T_{reg} populations from both L2/L2 and cKO mice promoted a significant reduction of colitis-induced *Tnfa* mRNA expression (fig. S9J). To exclude that the lack of protection by CD4$^+$ CD45Rb^{lo} cKO T cells was caused by a reduced frequency of T_{reg} in this population, we determined the percentage of splenic FoxP3$^+$ CD4$^+$ T cells in L2/L2 and cKO mice before transfer, revealing no difference (fig. S9K).

Impaired virus clearance by LRH-1–deficient cytotoxic T cells

The impact of LRH-1 deletion was more pronounced in regard to mature CD4$^+$ T cell numbers, while CD8$^+$ T lymphocytes were less affected. To investigate the effect of LRH-1 deletion on CD8$^+$ T cell effector functions, we analyzed the antigen-specific T cell expansion and viral clearance after lymphocytic choriomeningitis virus (LCMV) infection, which is critically dependent on cytotoxic CD8$^+$ T cells (*26*). Accordingly, LCMV infection resulted in increased numbers of splenic CD8αβ$^+$ αβ T cell receptor–positive (TCRαβ$^+$) cells in L2/L2 mice at day 6 after LCMV infection, indicative of a virus-specific T cell expansion. Although cKO mice had lower numbers of CD8αβ$^+$ TCRαβ$^+$

cells before infection, a clear virus-induced expansion was observed at days 6 and 8 after infection (Fig. 6A). Along with the virus-induced cytotoxic T cell expansion, an increase in $CD69^+$ and $CD25^+$ $CD8^+$ T cells was observed at day 6 after infection; however, no difference was seen between L2/L2 and cKO mice (Fig. 6, B and C). Similarly, a comparable virus-induced increase of $CD25^+$ $CD8^+$ T cells in mesenteric lymph nodes was observed (fig. S10A). The expansion of virus-specific T cells was confirmed using intracellular staining of IFN-γ. While only ex vivo restimulation with the LCMV peptide gp33, but not the control peptide adn5, resulted in IFN-γ^+ $CD8^+$ T cells at days 6 and 8 after infection, no difference was seen between control and cKO mice (Fig. 6D). Similar observations were made when analyzing IFN-γ levels in serum samples (fig. S10B). Thus, LRH-1 deficiency does not appear to affect LCMV-induced $CD8^+$ T cell activation and expansion.

An important effector function of virus-specific T cells is the killing of virus-infected cells and, thereby, virus clearance. Accordingly, a massive reduction of virus particles was seen in the spleen, liver, small intestine, and serum of LCMV-infected control mice at day 10 after infection (Fig. 6, E to H). However, while $CD8^+$ cKO T cells appeared to become properly activated and expand after LCMV infection, they completely failed to control viral expansion,

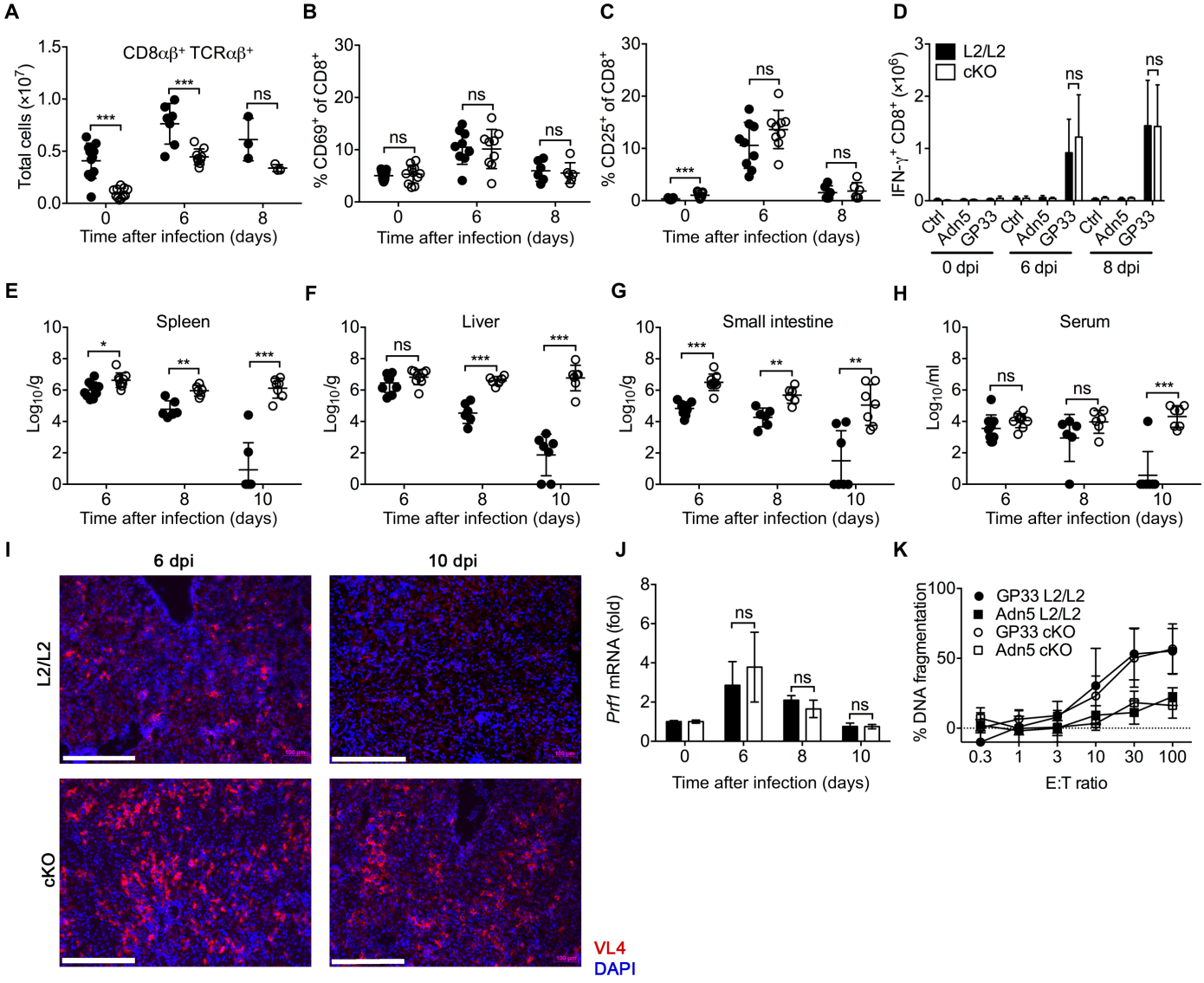

Fig. 6. Impaired virus clearance by LRH-1–deficient cytotoxic T cells. (**A**) Virus-induced expansion of $CD8\alpha\beta^+$ $TCR\alpha\beta^+$ T cells [0 days post infection (dpi), $n = 11$; 6 dpi, $n = 9$; 8 dpi, $n = 3$ mice]. (**B** and **C**) Up-regulation of activation marker CD69 (B) and CD25 (C) in $CD8^+$ T cells after LCMV infection (0 dpi, $n = 11$; 6 dpi, $n = 9$; 8 dpi, $n = 6$ mice). (**D**) Quantification of IFN-γ–producing virus-specific $CD8^+$ T cells after ex vivo restimulation with buffer control, Adn5 control peptide or GP33 peptide (0 dpi: $n = 8$; 6 dpi: $n = 9$; 8 dpi: $n = 6$ mice). (**E** to **H**) Virus titers after LCMV infection of L2/L2 or cKO mice in the spleen (E), liver (F), small intestine (G), and serum (H) (6 dpi, $n = 9$; 8 dpi, $n = 6$; 10 dpi, $n = 7$ mice). (**I**) Immunohistological detection of LCMV-infected cells in liver sections in L2/L2 or cKO mice at days 6 and day 10 after infection. VL4 LCMV nucleoprotein, red; nuclei, blue (DAPI). Representative pictures are shown. Scale bars, 150 μm. (**J**) mRNA expression of the cytotoxic T cell effector molecule perforin (*Prf1*) (0 dpi, $n = 5$; 6 dpi, $n = 5$; 8 dpi, $n = 6$; 10 dpi, $n = 2$ mice). (**K**) DNA fragmentation of GP33 or Adn5-loaded EL4 cells by virus-specific T cells, 8 days after LCMV infection, measured by loss of ^{3}H-thymidine ($n = 3$ mice; representative experiment of two is shown). $^*P < 0.05$, $^{**}P < 0.01$, $^{***}P < 0.001$. E:T, effector:target.

resulting in a high viral load in all tissues examined (Fig. 6, E to H). The lack of viral clearance was also obvious when detecting LCMV-infected cells in liver tissue using immunofluorescence. While control mice almost completely cleared the virus from liver tissue at day 10 after infection, cKO mice still contained high numbers of virus-producing hepatocytes (Fig. 6I). As LCMV clearance is critically dependent on perforin-mediated cytotoxicity (*27*), we analyzed *Prf1* and *Gzmb* mRNA expression in the spleen of control and cKO mice, revealing an infection-induced increase in both mouse lines (Fig. 6J and fig. S10C). Furthermore, spleen cells and sorted $CD8^+$ T cells from both virus-infected control and cKO mice killed LCMV peptide–presenting target cells equally well (Fig. 6K and fig. S10D). This indicates that impaired expression of cytotoxic effector molecules is not responsible for the inability of cKO T cells to clear LCMV.

DISCUSSION

The expression and role of LRH-1 has been well described in various endodermal tissues, while considerably less is known about its expression and role in other tissues, specifically the hematopoietic system. The first indirect report investigating the LRH-1 expression in pancreatic tumors, where they accidentally observed LRH-1–positive tumor-infiltrating leukocytes, came from Benod and colleagues (*28*). More recently, Lefèvre *et al.* (*15*) described LRH-1 expression in macrophages and a role of LRH-1 in cytokine-induced differentiation. Our own studies revealed a role of LRH-1 in the transcriptional control of Fas ligand expression in $CD4^+$ T cells (*16*). However, besides these few studies, the expression and role of LRH-1 in the hematopoietic system is currently unexplored. One of the underlying reasons seems to be that steady-state levels are extremely low; thus, LRH-1 expression and function in immune cells had been largely ignored. We observed that expression levels in unstimulated thymocytes and mature T cells are about 100 to 1000 times lower than those observed in the intestine and the liver (fig. S1, A to D). However, LRH-1 expression in T cells appears to be rather dynamic. Activation of T cells by mitogenic stimuli strongly induces LRH-1 promoter activity, expression, and function (Fig. 3, A, B, D, and F). LRH-1 induction by mitogenic stimuli correlates well with the up-regulation of cell cycle–regulating genes, i.e., c-Myc and cyclin E1 (Fig. 3, C to E). This is in line with the established role of LRH-1 in the transcriptional control of these cyclin genes and the regulation of proliferation of intestinal epithelial stem cells and tumor cells (*19*). Supporting a suggested role of LRH-1 in cell cycle progression, we observed a profound inhibition of activation-induced proliferation when LRH-1 was either genetically deleted or pharmacologically inhibited (Fig. 4, A to F). Reduced proliferation was observed not only in vitro but also during homeostatic expansion in vivo (fig. S7, A and B) and the pathogenesis of experimental colitis (Fig. 5, A to G). This proliferation deficiency is unlikely a consequence of improper T cell activation, as LRH-1–deficient T cells readily up-regulated early activation markers (Fig. 2, A and B), and levels of IL-2 and IFN-γ produced often exceeded those of control T cells (Fig. 2, C and D). Given the previously described role of LRH-1 in the transcriptional regulation of cell cycle–related genes, e.g., cyclin D1 and E1 and c-Myc, in the liver and intestinal epithelial cells (*19*), the lack of LRH-1 very likely leads to defects in activation-induced proliferation in T cells due to reduced expression of these LRH-1 target genes. We have seen that cyclin E1 (*Cdne1*) and c-Myc (*Myc*) are expressed at reduced levels in LRH-1–deficient T cells (Fig. 4, G and H).

Unexpectedly, we observed quite substantial differences between the impact of LRH-1 deletion on $CD4^+$ versus $CD8^+$ T cells (Fig. 1, D, H, and I). While LRH-1 deletion resulted in a threefold reduction of mature peripheral $CD4^+$ T cells, $CD8^+$ T cells were only reduced by half (Fig 1, H and I). Similarly, activation-induced proliferation of $CD8^+$ T cells appeared to be less dependent on LRH-1, as in a mixed spleen cell population $CD8^+$ T cells divided normally in response to TCR stimulation, while $CD4^+$ were severely impaired (Fig. 4, A and B). During homeostatic T cell expansion in vivo, LRH-1–deficient $CD8^+$ T cells barely differed from wild-type T cells, while LRH-1–deficient $CD4^+$ T cells were not able to compete with wild-type T cells in repopulating $Rag1^{-/-}$ recipients (fig. S7, A and B). In addition, during LCMV infection, a normal expansion of LRH-1–deficient virus-specific $CD8^+$ T cells was observed, although they started at a lower level (Fig. 6A). As the CD4 promoter becomes activated already at the double-positive stage during thymic maturation, the LRH-1 gene is already deleted at this stage of T cell development (fig. S4, A to D). As CD4 promoter activity drops in mature $CD8^+$ T cells, an insufficient duration of Cre expression and associated failure to completely delete the LRH-1 gene could account for the reduced impact of LRH-1 deletion in $CD8^+$ T cells. However, the use of the mTmG double-fluorescent reporter mouse revealed efficient Cre-mediated conversion of tdTomato-positive to GFP-positive cells in both $CD4^+$ and $CD8^+$ T cell populations, although Cre-mediated excision appeared to be slightly more efficient in $CD4^+$ T cells (fig. S4, F to H). Nonetheless, it is unlikely that incomplete LRH-1 deletion accounts for the differences in proliferation observed, as the vast majority of LRH-1–deficient $CD8^+$ T cells were also GFP^+, indicating a sufficient phase of active Cre recombinase during their development. The difference in LRH-1 dependency between $CD4^+$ and $CD8^+$ T cells may be rather related to the presence or absence of compensatory signals. LRH-1–deficient $CD8^+$ T cells showed proliferation defects only when highly purified (Fig. 4F) but not when stimulated in the presence of antigen-presenting cells (Fig. 4, B and D). Thus, costimulatory signals distinct from B7-CD28 interaction may provide compensatory signals, enabling LRH-1–independent proliferation.

Defects in $CD4^+$ T cell proliferation correlated well with the inability of LRH-1–deficient $CD45RB^{hi}$ $CD4^+$ T cells to promote inflammation in the transfer model of colitis (Fig. 5, A to H). Similarly, the LRH-1–deficient T_{regs} in the $CD45RB^{lo}$ $CD4^+$ T cell population also failed to expand in vivo and to mediate protection from colitis induction (fig. S9, A to G). This inability to prevent transfer colitis is not due to a generally reduced level of T_{regs}, as the percentage of $FoxP3^+$ T_{regs} among splenic $CD4^+$ T cells was similar in control and LRH-1–deficient mice (fig. S9K). Thus, this rather suggests that in vivo proliferation of $CD4^+$ T_{regs} is also critically controlled by LRH-1. A somewhat different situation was observed in the LCMV infection model. Although T cell–specific LRH-1–deficient mice had generally lower numbers of $CD8^+$ T cells before infection, LCMV promoted a rapid expansion of virus-specific T cells even in the absence of LRH-1, as seen by a general increase in $CD8^+$ $TCR\alpha\beta^+$ T cells in the spleen (Fig. 6A) and lymph nodes (fig. S10A) and comparable numbers of IFN-γ–producing $CD8^+$ T cells upon ex vivo restimulation with the LCMV-specific peptide gp33 (Fig. 6D). Also along these lines, comparable production of cytokines and an increase in activation marker–positive (CD25 and CD69) $CD8^+$ T cells were observed (Fig. 6, B and C, and fig. S10B). In marked contrast, LRH-1–deficient cytotoxic T cells failed to control viral

spreading. While in control animals LCMV titers were reduced at day 10 after infection by several logs and barely detectable, viral titers in mice with defective LRH-1 expression remained at a high level (Fig. 6, E to I). Given that virus-specific T cells appeared to expand normally, this difference is difficult to reconcile. An obvious guess would be that LRH-1–deficient $CD8^+$ T cells fail to express cytotoxic effector molecules. However, gene expression analysis revealed that granzyme B and perforin are, at least on an mRNA level, induced upon viral infection and equally expressed in control and cKO mice (Fig. 6J and fig. S10C). While we have recently identified the cytotoxic effector molecule Fas ligand as a target gene of LRH-1 (*16*), it is unlikely that impaired Fas ligand expression could account for inefficient viral clearance, as perforin (*27*) but not Fas ligand (*29*) is critical for controlling LCMV spreading. Furthermore, we confirmed that T cells from both virus-infected control and cKO mice killed LCMV peptide–presenting target cells equally well, suggesting normal cytotoxic effector functions in both mouse lines.

Thus, alternative mechanisms have to be considered for the inefficiency of cKO mice to control LCMV. A possible explanation is that $CD8^+$ cells expand but cannot reach critical numbers to efficiently eliminate LCMV. Another possibility is that cKO T cells are more readily exhausted and thereby cannot control viral expansion. Alternatively, an efficient cytotoxic T cell response may also depend on proper T helper cell responses, which is likely impaired in cKO mice with reduced proliferative potential of $CD4^+$ T cells. In support of this hypothesis, it was reported that $CD4^+$ T cell help was required for effective $CD8^+$ T cell–mediated resolution of LCMV infection (*30*). Thus, T helper cells have been shown to critically orchestrate expansion and recruitment of cytotoxic $CD8^+$ T cells [reviewed in (*31*)].

An interesting aspect of our study is its potential translational application. Although no endogenous ligands for LRH-1 have been identified yet, a number of pharmacological inhibitors with high specificity have been developed. The fact that transient inhibition of LRH-1 with two inhibitors that act in different mechanisms [3d2 (Fig. 4, C and D) (*20*) and SR1848 (Fig. 4, E and F) (*21*)] was able to confirm that the proliferation-regulating role of LRH-1 in T cells and the relatively low expression of LRH-1 in comparison to the liver and intestine may open an interesting therapeutic window. The use of LRH-1 inhibitors in relatively low doses could permit the efficient inhibition of T cell mediated immunopathologies while not affecting vital functions of other tissues. While studying the role of LRH-1 in the transcriptional control of Fas ligand, we were already able to provide proof of principle for this concept. Injection of the lectin ConA into mice leads to rapid T cell activation and Fas ligand–dependent damage of the liver, which was strongly reduced after administration of 3d2 (*16*). The liver seems to tolerate 3d2 relatively well, as only a minimal increase in 3d2-induced serum transaminases was observed.

In summary, we have described a novel role for LRH-1 in T cell development, proliferation, and effector functions. Furthermore, our study proposes LRH-1 as an emerging new target in the treatment of T cell–mediated inflammatory diseases.

MATERIALS AND METHODS

Mice

Animals were housed in individually ventilated cages at the central animal facility of the University of Konstanz. Male and female mice aged 7 to 15 weeks on C57BL/6 background carrying the leukocyte marker CD45.2 were used for all in vitro and in vivo experiments unless otherwise stated. For mRNA quantitation experiments, wild-type C57BL/6 mice were used. $Nr5a2^{L2/L2}$ (L2/L2) mice (*9*) were bred with CD4-Cre transgenic mice (*32*) to obtain $Nr5a2^{L2/L2}$ CD4-Cre (cKO) animals and kept heterozygous for Cre expression. The Cre-reporter mTmG transgenic mice were provided by U. Koch (École Polytechnique Fédérale de Lausanne) and crossed with $Nr5a2^{L2/L2}$ CD4-Cre to obtain $Nr5a2^{L2/L2}$ mTmG CD4-Cre mice. Throughout all experiments, cKO animals were compared to their corresponding floxed littermate controls. Ly5.1 mice expressed the leukocyte marker CD45 isoform 1. $Rag1^{-/-}$ (provided by M. Basler, University of Konstanz) mice were bred on a Ly5.1 background.

Cell culture and reagents

All experiments were performed in 96-well round-bottom plates (Greiner) in technical triplicates with 200,000 cells per well in complete culture medium unless otherwise stated. Cell culture media and supplements were purchased from Sigma-Aldrich, if not otherwise indicated.

Human leukemic Jurkat cells (the American Type Culture Collection) with stably transfected SV40 large T antigen (lT) were maintained in RPMI 1640 medium supplemented with 5% fetal calf serum (FCS), 2 mM L-glutamine, and gentamycin (20 μg/ml) at 37°C and 5% CO_2. Cells have been routinely tested for the absence of mycoplasma. Mouse T cells were cultured in RPMI 1640 medium supplemented with 10% FCS, 2 mM L-glutamine, gentamycin (20 μg/ml), and 50 μM β-mercaptoethanol.

Luciferase reporter assay

The 1.5-kb human LRH-1 promoter luciferase reporter and control constructs have been described previously (*33*). Jurkat lT cells were transfected by nucleofection (Amaxa) (*16*), seeded at a concentration of 3×10^5 cells/ml in 12-well plates, and cultured overnight before treatment with phorbol myristate acetate (PMA) (50 ng/ml) and ionomycin (1.1 μg/ml) (both from Enzo Life Sciences) or serum withdrawal for further 24 hours. Luciferase assays were carried out as described previously (*34*). Chemiluminescence was measured using an Infinite 200 PRO (Tecan) microplate reader. pCMV β-galactosidase was used to correct for transfection efficiencies. To test endogenous LRH-1 activity, Jurkat lT cells were transfected with a luciferase reporter construct containing 5× LRH-1 response elements derived from the small heterodimer partner promoter (*35*).

T cell isolation and activation

Single-cell suspensions from the spleen, thymus, and lymph nodes were prepared by manual disruption between frosted glass slides. Human PBMCs were prepared by Ficoll density centrifugation.

For *Nr5a2* mRNA quantitation experiments, freshly isolated splenocytes were stimulated with 5 μg/ml ConA (Sigma-Aldrich) or PMA (5 ng/ml) and ionomycin (200 ng/ml) for 3 hours and immediately frozen in appropriate reagents for subsequent mRNA analysis. Alternatively, cells were activated with anti-CD3ε antibody (3 μg/ml) (clone 145-2C11) and precoated on 96-well flat bottom plates in 50 mM tris (pH 9) and soluble purified anti-CD28 antibody (1 μg/ml) (BioLegend). ConA-activated mouse splenocytes were prepared as a source of T cell blasts and cultured as described (*16*). Human PBMC

were treated with phytohemagglutinin (5 μg/ml) (Sigma-Aldrich) for 3 hours before RNA isolation.

RNA isolation and real time quantitative polymerase chain reaction

Tissue RNA was isolated using peqGOLD TriFast (Peqlab) according to the manufacturer's instructions. For sorted cells, the ReliaPrep RNA Mini Kit (Promega) was used. Complementary DNA (cDNA) was prepared using the High-Capacity cDNA Reverse Transcription Kit (Applied Biosystems). Quantitative polymerase chain reaction (PCR) was performed on a StepOnePlus Instrument using SYBR Green PCR Master Mix (both from Applied Biosystems). Primers were designed to span exon-exon junctions. Gene expression was normalized to *Actb* or *GAPDH*, respectively. The following primers were used: *Nr5a2*, 5′-TTGAGTGGGCCAGGAGTAGT-3′ (forward) and 5′-ACGCGACTTCTGTGTGTGAG-3′ (reverse); *Actb*, 5′-TATTGGCAACGAGCG GTTCC-3′ (forward) and 5′-GCACTGTGTTGGCATAGAGG-3′ (reverse); *Myc*, 5′-CTAGTGCTGCATGAGGAGAC-3′ (forward) and 5′-TTTGCCTCTTCTCCACAGAC-3′ (reverse); *Cdne1*, 5′-TTCTGCAGCGTCATCCTCTC-3′ (forward) and 5′-TGTGCCAAGTAGAACGTCTC-3′ (reverse); *Tnfa*, 5′-TAGCCCACGTCGTAGCAAAC-3′ (forward) and 5′-ACAAGGTACAACCCATCGGC-3′ (reverse); *Il1b*, 5′-TGCCACCTTTTGACAGTGATG-3′ (forward) and 5′-ATGTGCTGCTGCGAGATTTG-3′ (reverse); *Ifng*, 5′-CGGCACAGTCATTGAAAGCC-3′ (forward) and 5′-TGTCACCATCCTTTTGCCAGT-3′ (reverse); *Prf1*, 5′-TCTTGGTGGGACTTCAGCTTT-3′ (forward) and 5′-TCCATACACCTGGCACGAAC-3′ (reverse); *Gzmb*, 5′-GCTGCTAAAGCTGAAGAGTAAGG-3′ (forward) and 5′-TCACATTGACATTGCGCCTG-3′ (reverse); human *NR5A2*, 5′-GGGCAACAAGTGGACTATTC-3′ (forward) and 5′-CCAGCTGGAAGTTTTCAAGG-3′ (reverse); and human *GAPDH*, 5′-ATGGAGAAGGCTGGGGCTCA-3′ (forward) and 5′-AGTGATGGCATGGACTGTGGTCAT-3′ (reverse).

Flow cytometry and cell sorting

Single-cell suspensions of freshly isolated T cells were stained with one or more of the following monoclonal antibodies: anti–CD3ε-APC (anaphase-promoting complex) (145-2C11), anti–CD8-PE (phycoerythrin) (53-6.7), anti–CD45.1-BV421 (A20), anti–CDCD45.2-APC (104), anti–CD4-FITC (fluorescein isothiocyanate) (RM4-5), and anti–CD8α–PerCP-Cy5.5 (53-6.7) from BD Pharmingen; anti–CD4-Cy5 (GK1.5), anti–CD25-APC (PC61.5), anti–F4/80-APC (BM8), anti–NK1.1-PE (PK136), anti–CD45R (B220)–PerCP-Cy5.5 (RA3-6B2), anti–CD4-PE (GK1.5), anti–CD8β-FITC (eBioH35-17.2), anti–FoxP3-PE (FJK-16s), and anti–TCRβ-PE-Cy7 (H57-597) from eBioscience; anti–IFN-γ–FITC (XMG1.2) and anti–CD69-PE (H1.2F3) from BioLegend; and anti–CD3ε-FITC (145-2C11; purified from culture supernatant); anti-VL4 antibody was a gift from M. Basler (University of Konstanz). The following polyclonal secondary antibodies were used: goat anti-rat immunoglobulin G (IgG)–Alexa Fluor 568 (Invitrogen) and goat anti-hamster IgG-FITC cocktail (G70-204/G94-56, BD Pharmingen). Flow cytometry was performed on an LSRFortessa (BD Biosciences). For cell sorting, an Aria III (BD Biosciences) instrument was used. Data were analyzed using FlowJo software (TreeStar).

For intracellular cytokine staining, cells were restimulated in vitro with gp33 peptide (1 μg/ml) (KAVYNFATC) or adn5 control peptide (SGPSNTPPEI; both from ProImmune) and incubated with brefeldin A (10 μg/ml) (LKT Labs) for 5 hours. Staining (anti–CD8-PE and anti–IFN-γ–FITC) was performed as described before (*36*). For detection of T_{regs}, splenocytes were surface-stained with anti–CD4-FITC before they were stained intracellularly with anti–FoxP3-PE using the Fix/Perm Kit (BioLegend).

Histology and immunohistochemistry

Mouse colons and small intestinal segments were swiss-rolled and fixed in 10% formalin, followed by paraffin embedding. Tissue sections (4 μm) were stained with hematoxylin and eosin for histological analysis using standard procedures.

For immunohistochemistry, organs were immediately embedded in O.C.T. (Tissue-Tek) cryosection medium and shock frozen on dry ice. Sections (7 μm) were cut, and samples were fixed with fresh acetone for 1 min, treated with anti-CD16/32 Fc-block, stained with appropriate antibodies, and detected with Alexa Fluor 568– and FITC-conjugated secondary antibodies. mTmG cryosections were directly analyzed without further processing. All sections were embedded in 4′,6-diamidino-2-phenylindole containing Fluoroshield (Sigma-Aldrich) and analyzed on an Axio Observer Z1 (Zeiss) microscope. Fiji software (*37*) was used for image processing.

Cell death assays

Isolated T cells were cultured in the presence or absence of dexamethasone (Sigma-Aldrich), etoposide (Enzo Life Sciences), staurosporine (Sigma-Aldrich), plate bound anti-CD3 antibody, or solvent control (dimethyl sulfoxide or ethanol) for 8 hours. Cells were counterstained with anti–CD4-Cy5 and anti–CD8-PE in binding buffer and analyzed for annexin-V positivity, as described (*38*).

Proliferation assays

Lymphocyte proliferation was monitored using CFSE (Sigma-Aldrich) dilution, as described (*39*). Cells were counterstained with anti–CD4-Cy5 and anti–CD8-PE and analyzed by flow cytometry. In some experiments, the pharmacological LRH-1 inhibitor 3d2 (*20*), control substance cd7 (*20*) (both synthesized by ChemBridge Corporation), or SR1848 (*21*) were added 30 min before T cell activation.

For ^{3}H-thymidine incorporation assays, cells were pulsed with 0.5 μCi ^{3}H-thymidine (Hartmann Analytic) per well for 18 hours and harvested using a semiautomated cell harvester (Packard). ^{3}H-thymidine integration was determined by scintillation counting. For cell cycle profile analysis, wild-type splenocytes were cultured for indicated time points before nuclear DNA content was analyzed as described earlier (*40*).

Analysis of cytokine expression and serum immunoglobulin titers

Secretion of murine IL-2 and IFN-γ was quantified by enzyme-linked immunosorbent assay (ELISA) using matched antibody pairs [anti-mouse IFN-γ (RA-6A2/XMG1.2) and anti-mouse IL-2 (JES6-1A12/JES6-5H4)]. All reagents were purchased from BioLegend and used according to the manufacturer's instructions.

For the determination of anti-ovalbumin–specific IgG antibodies in mouse serum, polystyrene microtiter plates (Nunc) were coated with ovalbumin (100 μg/ml) and horseradish-conjugated goat anti-mouse IgG (Jackson ImmunoResearch) was used for detection.

Ovalbumin immunization and in vitro restimulation

Mice were subcutaneously injected with 100 μg of ovalbumin emulsified in incomplete Freund's adjuvant (Invivogen). After 14 days,

the spleen and serum were isolated for further analysis of antibody production by ELISA and proliferation of antigen-specific T cells by in vitro restimulation and ^{3}H-thymidine incorporation.

Adoptive transfer studies

Isolated splenocytes were sorted accordingly on the basis of CD4 and CD8α staining. A minimal purity of 98% was confirmed, and appropriate cell populations were mixed in a 1:1 ratio. A total of 2×10^6 cells were intraperitoneally injected into Rag1$^{-/-}$ recipient mice. Animals were euthanized 21 days after injection, and secondary lymphatic organs were analyzed for T cell numbers, subsets, and origin (CD45.1 versus CD45.2).

Transfer colitis and protection

Splenocytes were sorted on the basis of CD4-PE and CD45Rb-FITC staining for CD4$^+$ CD45RB^{hi} and CD4$^+$ CD45RB^{lo}, as described previously (*23*). A minimum purity of 98% was ensured. For the induction of transfer colitis, Rag1$^{-/-}$ received 0.5×10^6 CD45Rb^{hi} cells from either L2/L2 or cKO mice by intraperitoneal injection. For transfer colitis protection experiments, Rag1$^{-/-}$ animals were intraperitoneally injected with 0.5×10^6 CD4$^+$ CD45Rb^{hi} cells from Ly5.1 donor mice and 0.25×10^6 CD4$^+$ CD45Rb^{lo} T cells from either L2/L2 or cKO mice. In both experiments, body weight was recorded to monitor disease progression and estimate colitis severity. Animals were euthanized once most of the mice reached a critical weight loss of 20%. Cells from secondary lymphatic organs were isolated, stained for CD4 and CD45.1, and analyzed by flow cytometry. CD4$^+$ CD45.1$^-$ cells were considered as repopulating donor T cells.

LCMV infection and virus-specific T cell cytotoxicity

Mice were intravenously injected with 2.5×10^5 plaque-forming units of LCMV strain WE in phosphate-buffered saline and euthanized at day 6, 8, or 10, respectively. For characterization and intracellular staining, T cells were isolated from spleen and mesenteric lymph node and stained as described above. Virus titers were analyzed in different organs using plaque assay, as described previously (*41*). For the detection of virus-specific cytotoxic T cells, EL4 thymoma cells were labeled with ^{3}H-thymidine (10 μCi/ml) overnight and pretreated with gp33 or adn5 peptide. Effector cells were mixed with 2×10^4 target cells in triplicate at the indicated effector:target ratio for 16 hours before the ^{3}H-thymidin content was determined by scintillation counting. DNA fragmentation was calculated as previously described (*16*).

Study approval

All animal experiments were performed in accordance with German animal experimentation regulations approved by the Ethics Review Board of the Regierungspräsidium Freiburg. The G*Power software was used to predetermine sample size of all animal experiments.

Statistics

Values reported are means ± SD. Statistical significance was determined by unpaired two-tailed Student's *t* test using Prism (version 6.0b, GraphPad). Where indicated, one-way analysis of variance (ANOVA) with Bonferroni's multiple comparisons test was used. *P* values are indicated as follows: $^*P < 0.05$, $^{**}P < 0.01$, and $^{***}P < 0.001$. Confidence interval was set to 95%.

SUPPLEMENTARY MATERIALS

Supplementary material for this article is available at http://advances.sciencemag.org/cgi/content/full/5/7/eaav9732/DC1

Fig. S1. *Nr5a2* expression in immature and mature T lymphocytes.
Fig. S2. Minor impact of *Nr5a2* deletion on immature T lymphocytes.
Fig. S3. Reduced mature T cells in axial and mesenteric lymph nodes of LRH-1–deficient mice.
Fig. S4. Efficiency of LRH-1 deletion in immature and mature T cells.
Fig. S5. Apoptosis induction in LRH-1–deficient thymocytes.
Fig. S6. Apoptosis induction in LRH-1–deficient splenocytes.
Fig. S7. Homeostatic expansion is impaired in LRH-1–deficient T cells.
Fig. S8. Impaired ovalbumin-induced T cell expansion and antibody production in LRH-1–deficient mice.
Fig. S9. Reduced T_{regs} function of LRH-1–deficient T cells.
Fig. S10. Activation and cytotoxicity of LRH-1–deficient CD8$^+$ T cells.

REFERENCES AND NOTES

1. S. M. Innis, Dietary lipids in early development: Relevance to obesity, immune and inflammatory disorders. *Curr. Opin. Endocrinol. Diabetes Obes.* **14**, 359–364 (2007).
2. Y. Sanz, A. Moya-Pérez, Microbiota, inflammation and obesity. *Adv. Exp. Med. Biol.* **817**, 291–317 (2014).
3. C. McKenzie, J. Tan, L. Macia, C. R. Mackay, The nutrition-gut microbiome-physiology axis and allergic diseases. *Immunol. Rev.* **278**, 277–295 (2017).
4. P. C. Calder, Long chain fatty acids and gene expression in inflammation and immunity. *Curr. Opin. Clin. Nutr. Metab. Care* **16**, 425–433 (2013).
5. M. K. Crowder, C. D. Seacrist, R. D. Blind, Phospholipid regulation of the nuclear receptor superfamily. *Adv. Biol. Regul.* **63**, 6–14 (2017).
6. T. J. Cole, Glucocorticoid action and the development of selective glucocorticoid receptor ligands. *Biotechnol. Annu. Rev.* **12**, 269–300 (2006).
7. M. Noti, D. Sidler, T. Brunner, Extra-adrenal glucocorticoid synthesis in the intestinal epithelium: More than a drop in the ocean? *Semin. Immunopathol.* **31**, 237–248 (2009).
8. I. Cima, N. Corazza, B. Dick, A. Fuhrer, S. Herren, S. Jakob, E. Ayuni, C. Mueller, T. Brunner, Intestinal epithelial cells synthesize glucocorticoids and regulate T cell activation. *J. Exp. Med.* **200**, 1635–1646 (2004).
9. A. Coste, L. Dubuquoy, R. Barnouin, J.-S. Annicotte, B. Magnier, M. Notti, N. Corazza, M. C. Antal, D. Metzger, P. Desreumaux, T. Brunner, J. Auwerx, K. Schoonjans, LRH-1-mediated glucocorticoid synthesis in enterocytes protects against inflammatory bowel disease. *Proc. Natl. Acad. Sci. U.S.A.* **104**, 13098–13103 (2007).
10. M. Mueller, I. Cima, M. Noti, A. Fuhrer, S. Jakob, L. Dubuquoy, K. Schoonjans, T. Brunner, The nuclear receptor LRH-1 critically regulates extra-adrenal glucocorticoid synthesis in the intestine. *J. Exp. Med.* **203**, 2057–2062 (2006).
11. M. Noti, N. Corazza, C. Mueller, B. Berger, T. Brunner, TNF suppresses acute intestinal inflammation by inducing local glucocorticoid synthesis. *J. Exp. Med.* **207**, 1057–1066 (2010).
12. E. Fayard, J. Auwerx, K. Schoonjans, LRH-1: An orphan nuclear receptor involved in development, metabolism and steroidogenesis. *Trends Cell Biol.* **14**, 250–260 (2004).
13. I. N. Krylova, E. P. Sablin, J. Moore, R. X. Xu, G. M. Waitt, J. A. Mackay, D. Juzumiene, J. M. Bynum, K. Madauss, V. Montana, L. Lebedeva, M. Suzawa, J. D. Williams, S. P. Williams, R. K. Guy, J. W. Thornton, R. J. Fletterick, T. M. Willson, H. A. Ingraham, Structural analyses reveal phosphatidyl inositols as ligands for the NR5 orphan receptors SF-1 and LRH-1. *Cell* **120**, 343–355 (2005).
14. E. A. Ortlund, Y. Lee, I. H. Solomon, J. M. Hager, R. Safi, Y. Choi, Z. Guan, A. Tripathy, C. R. H. Raetz, D. P. McDonnell, D. D. Moore, M. R. Redinbo, Modulation of human nuclear receptor LRH-1 activity by phospholipids and SHP. *Nat. Struct. Mol. Biol.* **12**, 357–363 (2005).
15. L. Lefèvre, H. Authier, S. Stein, C. Majorel, B. Couderc, C. Dardenne, M. A. Eddine, E. Meunier, J. Bernad, A. Valentin, B. Pipy, K. Schoonjans, A. Coste, LRH-1 mediates anti-inflammatory and antifungal phenotype of IL-13-activated macrophages through the PPARγ ligand synthesis. *Nat. Commun.* **6**, 6801 (2015).
16. J. Schwaderer, A.-K. Gaiser, T. S. Phan, M. Delgado, T. Brunner, Liver receptor homolog-1 (NR5a2) regulates CD95/Fas ligand transcription and associated T-cell effector functions. *Cell Death Dis.* **8**, e2745 (2017).
17. M. D. Muzumdar, B. Tasic, K. Miyamichi, L. Li, L. Luo, A global double-fluorescent Cre reporter mouse. *Genesis* **45**, 593–605 (2007).
18. P. H. Krammer, R. Arnold, I. N. Lavrik, Life and death in peripheral T cells. *Nat. Rev. Immunol.* **7**, 532–542 (2007).
19. O. A. Botrugno, E. Fayard, J.-S. Annicotte, C. Haby, T. Brennan, O. Wendling, T. Tanaka, T. Kodama, W. Thomas, J. Auwerx, K. Schoonjans, Synergy between LRH-1 and β-catenin induces G_1 cyclin-mediated cell proliferation. *Mol. Cell* **15**, 499–509 (2004).
20. C. Benod, J. Carlsson, R. Uthayaruban, P. Hwang, J. J. Irwin, A. K. Doak, B. K. Shoichet, E. P. Sablin, R. J. Fletterick, Structure-based discovery of antagonists of nuclear receptor LRH-1. *J. Biol. Chem.* **288**, 19830–19844 (2013).

21. C. A. Corzo, Y. Mari, M. R. Chang, T. Khan, D. Kuruvilla, P. Nuhant, N. Kumar, G. M. West, D. R. Duckett, W. R. Roush, P. R. Griffin, Antiproliferation activity of a small molecule repressor of liver receptor homolog 1. *Mol. Pharmacol.* **87**, 296–304 (2014).
22. L. Xiao, Y. Wang, W. Liang, L. Liu, N. Pan, H. Deng, L. Li, C. Zou, F. L. Chan, Y. Zhou, LRH-1 drives hepatocellular carcinoma partially through induction of c-myc and cyclin E1, and suppression of p21. *Cancer Manag. Res.* **10**, 2389–2400 (2018).
23. N. Corazza, S. Eichenberger, H.-P. Eugster, C. Mueller, Nonlymphocyte-derived tumor necrosis factor is required for induction of colitis in recombination activating gene (RAG)2$^{-/-}$ mice upon transfer of CD4^{+}CD45RB^{hi} T cells. *J. Exp. Med.* **190**, 1479–1492 (1999).
24. D. V. Ostanin, J. Bao, I. Koboziev, L. Gray, S. A. Robinson-Jackson, M. Kosloski-Davidson, V. H. Price, M. B. Grisham, T cell transfer model of chronic colitis: Concepts, considerations, and tricks of the trade. *Am. J. Physiol. Gastrointest. Liver Physiol.* **296**, G135–G146 (2009).
25. F. Powrie, T cells in inflammatory bowel disease: Protective and pathogenic roles. *Immunity* **3**, 171–174 (1995).
26. M. J. Buchmeier, R. M. Welsh, F. J. Dutko, M. B. A. Oldstone, The virology and immunobiology of lymphocytic choriomeningitis virus infection. *Adv. Immunol.* **30**, 275–331 (1980).
27. D. Kägi, B. Ledermann, K. Bürki, P. Seiler, B. Odermatt, K. J. Olsen, E. R. Podack, R. M. Zinkernagel, H. Hengartner, Cytotoxicity mediated by T cells and natural killer cells is greatly impaired in perforin-deficient mice. *Nature* **369**, 31–37 (1994).
28. C. Benod, M. V. Vinogradova, N. Jouravel, G. E. Kim, R. J. Fletterick, E. P. Sablin, Nuclear receptor liver receptor homologue 1 (LRH-1) regulates pancreatic cancer cell growth and proliferation. *Proc. Natl. Acad. Sci. U.S.A.* **108**, 16927–16931 (2011).
29. S. Balkow, A. Kersten, T. T. T. Tran, T. Stehle, P. Grosse, C. Museteanu, O. Utermöhlen, H. Pircher, F. von Weizsäcker, R. Wallich, A. Müllbacher, M. M. Simon, Concerted action of the FasL/Fas and perforin/granzyme A and B pathways is mandatory for the development of early viral hepatitis but not for recovery from viral infection. *J. Virol.* **75**, 8781–8791 (2001).
30. T. Trautmann, J.-H. Kozik, A. Carambia, K. Richter, T. Lischke, D. Schwinge, H.-W. Mittrücker, A. W. Lohse, A. Oxenius, C. Wiegard, J. Herkel, CD4^{+} T-cell help is required for effective CD8^{+} T cell-mediated resolution of acute viral hepatitis in mice. *PLOS ONE* **9**, e86348 (2014).
31. S. L. Swain, K. K. McKinstry, T. M. Strutt, Expanding roles for CD4^{+} T cells in immunity to viruses. *Nat. Rev. Immunol.* **12**, 136–148 (2012).
32. A. Wolfer, T. Bakker, A. Wilson, M. Nicolas, V. Ioannidis, D. R. Littman, C. B. Wilson, W. Held, H. R. MacDonald, F. Radtke, Inactivation of Notch1 in immature thymocytes does not perturb CD4 or CD8 T cell development. *Nat. Immunol.* **2**, 235–241 (2001).
33. J.-S. Annicotte, E. Fayard, G. H. Swift, L. Selander, H. Edlund, T. Tanaka, T. Kodama, K. Schoonjans, J. Auwerx, Pancreatic-duodenal homeobox 1 regulates expression of liver receptor homolog 1 during pancreas development. *Mol. Cell. Biol.* **23**, 6713–6724 (2003).
34. A. Alonso, J. J. Merlo, S. Na, N. Kholod, L. Jaroszewski, A. Kharitonenkov, S. Williams, A. Godzik, J. D. Posada, T. Mustelin, Inhibition of T cell antigen receptor signaling by VHR-related MKPX (VHX), a new dual specificity phosphatase related to VH1 related (VHR). *J. Biol. Chem.* **277**, 5524–5528 (2002).
35. A. G. Atanasov, D. Leiser, C. Roesselet, M. Noti, N. Corazza, K. Schoonjans, T. Brunner, Cell cycle-dependent regulation of extra-adrenal glucocorticoid synthesis in murine intestinal epithelial cells. *FASEB J.* **22**, 4117–4125 (2008).
36. M. Basler, J. Moebius, L. Elenich, M. Groettrup, J. J. Monaco, An altered T cell repertoire in MECL-1-deficient mice. *J. Immunol.* **176**, 6665–6672 (2006).
37. J. Schindelin, I. Arganda-Carreras, E. Frise, V. Kaynig, M. Longair, T. Pietzsch, S. Preibisch, C. Rueden, S. Saalfeld, B. Schmid, J.-Y. Tinevez, D. J. White, V. Hartenstein, K. Eliceiri, P. Tomancak, A. Cardona, Fiji: An open-source platform for biological-image analysis. *Nat. Methods* **9**, 676–682 (2012).
38. D. Kassahn, T. Brunner, N. Corazza, Distinct but complementary roles of Fas ligand and Bim in homeostatic T cell apoptosis. *Cell Cycle* **7**, 3469–3471 (2008).
39. B. J. C. Quah, H. S. Warren, C. R. Parish, Monitoring lymphocyte proliferation in vitro and in vivo with the intracellular fluorescent dye carboxyfluorescein diacetate succinimidyl ester. *Nat. Protoc.* **2**, 2049–2056 (2007).
40. A. Brockmann, T. Strittmatter, S. May, K. Stemmer, A. Marx, T. Brunner, Structure–function relationship of thiazolide-induced apoptosis in colorectal tumor cells. *ACS Chem. Biol.* **9**, 1520–1527 (2014).
41. C. Wasem, D. Arnold, L. Saurer, N. Corazza, S. Jakob, S. Herren, C. Vallan, C. Mueller, T. Brunner, Sensitizing antigen-specific CD8^{+} T cells for accelerated suicide causes immune incompetence. *J. Clin. Invest.* **111**, 1191–1199 (2003).

Acknowledgments: We thank A. Glöckner, J. Negrassus, and D. Eichbichler for expert technical help; A. Holz and H. Henseleit for animal caretaking; M. Basler for the VL4-antibody; U. Koch and F. Radtke for the mTmG reporter mouse; and M. Groetrupp for advice; S. Martin for stimulating discussions and suggestions. **Funding:** This work was supported by grants from the German Science Foundation (DFG) (BR 3369/4-1, INST 38/500-1, and INST 38/498-1) to T.B. C.S. was supported by a fellowship from the graduate school RTG1331 (supported by the DFG). J.H. was supported by a fellowship from the Chinese Scholarship Council, and S.M. was supported by a Carl Zeiss fellowship. **Author contributions:** C.S., A.-L.G., J.H., T.S., C.R., P.G.-B., M.E.D., T.S.P., S.M., C.Sch. and L.D. conducted experiments. C.S., T.S.P., and C.R. sorted cells. K.S. and N.C. provided valuable reagents and advised on the manuscript. C.S. and T.B. wrote the manuscript. T.B. supervised the project and finalized the manuscript. **Competing interest:** The authors declare that they have no competing interests. **Data and materials availability:** All data needed to evaluate the conclusions in the paper are present in the paper and/or the Supplementary Materials. The floxed LRH-1 mouse line can be provided by K.S. pending on scientific review and a completed material transfer agreement. Request for this mouse line should be submitted to K.S. (kristina.schoonjans@epfl.ch). Additional data related to this paper may be requested from the authors.

Submitted 6 November 2018
Accepted 12 June 2019
Published 17 July 2019
10.1126/sciadv.aav9732

Citation: C. Seitz, J. Huang, A.-L. Geiselhöringer, P. Galbani-Bianchi, S. Michalek, T. S. Phan, C. Reinhold, L. Dietrich, C. Schmidt, N. Corazza, M. E. Delgado, T. Schnalzger, K. Schoonjans, T. Brunner, The orphan nuclear receptor LRH-1/NR5a2 critically regulates T cell functions. *Sci. Adv.* **5**, eaav9732 (2019).